

ed very far into the sinusoidal lumen itself.

After only 15 minutes of hypoxia, striking alterations in cell structure were observed in centrilobular regions (Fig. 2b). Most prominent were bleb-like protrusions of hepatocyte plasma membrane and cytoplasm into the lumen of the sinusoids through fenestrations in the endothelium. Bile canaliculi were marginally more distended, and intercellular borders showed a general flattening of larger topological features and a fine surface granularity.

The projecting blebs remained connected to hepatocytes by slender necks, as demonstrated by thin-section electron microscopy (Fig. 2c). Bleb contents were variable. In most blebs, only amorphous granular material was observed. Others contained endoplasmic reticulum and glycogen rosettes; larger organelles, such as mitochondria and lysosomes, were absent. After 45 minutes of hypoxia, blebs covered both the sinusoidal and the intercellular surfaces of the hepatocytes, grossly distorting them (Fig. 2d). In addition, the endothelium was torn and fragmented.

Clearly, perfusion of isolated, hemoglobin-free liver at low flow rates produces anoxic stress only to that portion of the lobule near the central vein. In experiments in which flow was reduced further, the amount of injured tissue increased. However, the area most proximal to the terminal portal venule was consistently spared.

Plasma membrane alterations have been described in a number of organs, including liver, following cellular injury from anoxia and other causes (12). Formation of the membranous blebs closely resembles the structural changes produced in isolated hepatocytes by the cytoskeletal disrupters cytochalasin B and phalloidin (13). Thus, the structural perturbations observed in hypoxia may represent a failure of the cytoskeleton to maintain cell shape and volume. It is also possible that the blebs formed during hypoxia are in the process of budding off and being released into the circulation. This could represent the well-known release of enzymes by injured hepatic tissue.

JOHN J. LEMASTERS

Laboratories for Cell Biology,
Department of Anatomy, School of
Medicine, University of North
Carolina, Chapel Hill 27514

SUNGCHUL JI

RONALD G. THURMAN

Department of Pharmacology,
School of Medicine,
University of North Carolina

References and Notes

1. R. N. M. MacSween, P. P. Anthony, P. J. Scheuer, Eds., *Pathology of the Liver* (Churchill Livingstone, Edinburgh, 1979).
2. A. M. Rappaport, *Beitr. Pathol.* **157**, 215 (1976).
3. F. Schaffner and H. Popper, *Scand. J. Gastroenterol. Suppl.* **5**, 69 (1970); C. S. Lieber, L. M. DeCarli, E. Rubin, *Proc. Natl. Acad. Sci. U.S.A.* **72**, 437 (1975); L. Van Waes and C. S. Lieber, *Gastroenterology* **73**, 646 (1977).
4. L. Videla, J. Bernstein, Y. Israel, *Biochem. J.* **134**, 507 (1973); J. Bernstein, L. Videla, Y. Israel, *ibid.*, p. 515; R. G. Thurman, W. R. McKenna, T. B. McCaffrey, *Mol. Pharmacol.* **12**, 156 (1976); T. Yuki and R. G. Thurman, *Biochem. J.* **186**, 119 (1980).
5. Y. Israel et al., *Proc. Natl. Acad. Sci. U.S.A.* **72**, 1137 (1975).
6. S. Ji, J. J. Lemasters, R. G. Thurman, *FEBS Lett.* **113**, 37 (1980).
7. ———, *Pharmacol. Biochem. Behav. Suppl.* **13**, 41 (1980).
8. R. Scholz, W. Hansen, R. G. Thurman, *Eur. J. Biochem.* **38**, 64 (1973).
9. S. Ji, B. Chance, K. Nishiki, T. Smith, T. Rich, *Am. J. Physiol.* **52**, C144 (1979); S. Ji, G. Lüthen, M. Kessler, in *Advanced Technobiology*, B. Ryback, Ed. (Sijthoff & Noordhoff, Alphen aan den Rijn, Netherlands, 1979), pp. 237–268.
10. B. Chance, J. R. Williamson, D. Jamieson, B. Schoener, *Biochem. Z.* **341**, 357 (1965).
11. P. Motta and K. R. Porter, *Cell Tissue Res.* **148**, 111 (1974); P. Motta, *ibid.* **164**, 371 (1975); J. W. Grisham, W. Nopanitaya, J. Compagno, A. E. H. Nägel, *Am. J. Anat.* **144**, 295 (1975); W. Nopanitaya and J. W. Grisham, *Exp. Mol. Pathol.* **23**, 441 (1975).
12. B. F. Trump, P. J. Goldblatt, R. E. Stowell, *Lab. Invest.* **11**, 986 (1962); R. B. Jennings, H. M. Sommers, P. B. Herdson, J. P. Kaltenbach, *Ann. N.Y. Acad. Sci.* **156**, 61 (1969); B. F. Trump and A. U. Arstila, in *Pathobiology of Cell Membranes*, B. F. Trump and A. U. Arstila, Eds. (Academic Press, New York, 1975), pp. 1–103.
13. E. Weiss, I. Sterz, M. Frimmer, R. Kroker, *Beitr. Pathol.* **150**, 345 (1973); G. C. Godman, A. F. Miranda, A. D. Deitch, S. W. Tanenbaum, *J. Cell Biol.* **64**, 644 (1975); M. Prentki et al., *ibid.* **81**, 592 (1979).
14. We thank R. S. Shively and W. H. Billica for expert technical assistance and E. Lieth for help in the darkroom. Supported by the American Heart Association with funds contributed in part by the North Carolina Heart Association and by NIH grants AA-03624 and AA-04853. R.G.T. is the recipient of career development award AA-00033.

5 December 1980; revised 21 January 1981

Intrinsic Birefringence Signal Preceding the Onset of Contraction in Heart Muscle

Abstract. *An intrinsic birefringence signal with two components occurring before sarcomere shortening was measured in mammalian cardiac muscle. The second component was sensitive to the inotropic state of the muscle as affected by external calcium concentration and epinephrine but not by changes of resting length. The second component was absent in frog heart. These results suggest that the second component of the birefringence signal reflects the activity of the sarcoplasmic reticulum related to excitation-contraction coupling processes occurring prior to onset of contraction in mammalian cardiac muscle.*

Intrinsic birefringence signals with a time course similar to an action potential were first recorded in electrical eel electric organ and squid giant axon (1, 2). In skeletal muscles, in addition to the component of the birefringence signal accompanying the action potential, a second component occurred immediately after the action potential and prior to the onset of contraction (3, 4). This second component has been attributed to the activity of the sarcoplasmic reticulum (SR) prior to activation of contraction. In intact skeletal muscle fibers the time course of the second component of the birefringence signal is similar to signals obtained by using voltage-sensitive dyes (5, 6) or the metallochromic calcium-indicator dye arsenazo III (7).

In these studies we have investigated birefringence signals in two different types of hearts; one with extensively developed SR (rat, guinea pig, and cat) and the other with much smaller content of SR and no T-tubular system (frog atrium and ventricle). In rat, guinea pig, and cat ventricular muscle, we found two distinct components of an intrinsic birefringence signal which preceded the development of tension. The first com-

ponent occurred simultaneously with the upstroke of the action potential. The second component began after a delay with respect to the upstroke and was much larger and slower than the first. Both components preceded the onset of sarcomere motion as measured by scattered incandescent light or laser-diffraction pattern, or both. The amplitude and rate of rise of the second component was related to the inotropic state of the muscle as regulated by the external calcium concentration, $[Ca]_o$, and epinephrine, but not by variations of resting muscle length. In frog atrial and ventricular muscle the birefringence signal showed only the action potential-related first component, under all experimental conditions including variations of $[Ca]_o$ and addition of epinephrine or caffeine. We conclude that the second component of the birefringence signal represents a step in activation of contraction that is probably related to the Ca^{2+} -release process of the SR in mammalian heart muscle.

Papillary muscles or trabeculae carnae (60 to 300 μ m in diameter by 0.75 to 1.2 mm long) were dissected from the right ventricle of rat and guinea pig hearts and from the right ventricle and atrium of cat

heart. Muscles were attached to a tension transducer and were perfused in a chamber mounted horizontally on the stage of a Zeiss IM35 inverted microscope. Muscles were equilibrated in normal Tyrode's solution (136 mM NaCl; 5.4 mM KCl; 2.4 mM CaCl₂; 0.8 mM MgCl₂; 11.9 mM NaHCO₃; 0.42 mM NaH₂PO₄; 5.6 mM D-glucose; equilibrated with 95 percent O₂ and 5 percent CO₂ at pH 7.35) for 1 hour before the start of an experiment. Stimulation was carried out with Ag-AgCl electrodes placed adjacent to the muscle. The experiments were conducted at room temperature (23° to 25°C). Incandescent white light was focused from above by a primary lens and a ×40 water immersion objective (Zeiss, NA 0.75) onto the muscle. An adjustable field stop and a polarizer were placed between the primary lens and ×40 objective. The polarizer was oriented at 45° to the longitudinal axis of the muscle. The transmitted light was collected from below by a ×25 objective (Zeiss, NA 0.60), passed through an analyzer (second polarizer) oriented at 90° to the polarizer (unless otherwise stated), and impinged onto a photodiode (EG &

G: PV 215). The signal was processed by a high-gain current-to-voltage converter, analog track-and-hold circuit, and a signal averager (Tracor Northern, TN 1505). Tension was monitored simultaneously on an oscilloscope and on a strip chart recorder (MFE 1000).

Figure 1a shows the time course of the birefringence signal (O_b) compared with the signal obtained from the impermeant membrane potential sensitive dye WW 444 (8) in a rat ventricular trabeculae. Developed tension and the scattered light were also measured. The first component of the birefringence signal (between arrows) had a time course simultaneous with the upstroke of the action potential (also between arrows) as measured by the WW 444 dye signal. Figure 1a also shows that, unlike the dye signal, the birefringence signal contains a second component. This second component is larger than, and in the same direction as, the first and occurs before the rapid change in scattered light induced by sarcomere motion or onset of contraction. The rate of rise of the second component was always slower than the first (upstroke-related) component. The distur-

tion caused by motion was too severe to monitor the full time course of the birefringence signal. Note that the contraction-induced distortion can also be seen in the voltage-sensitive dye trace (WW 444).

Figure 1b shows that the first and second components of the birefringence signal have characteristics that are most consistent with a change in optical retardation (9). The birefringence signal obtained with the polarizer and analyzer axes in parallel (trace O_p) is compared with the birefringence signal when polarizer and analyzer axes are at 90° to each other (trace $-O_b$, electronically inverted for convenience). Note that the two traces are virtually superimposable until the onset of movement artifact. This experiment shows that the decrease in retarded light (trace $-O_b$) was also measurable as an increase, of equal magnitude, in nonretarded light even though the resting light intensities for the two traces were different (see Fig. 1b).

Experiments were also performed to define the interval in which optical signals occur free of movement artifact. Changes in the zero- and first-order laser

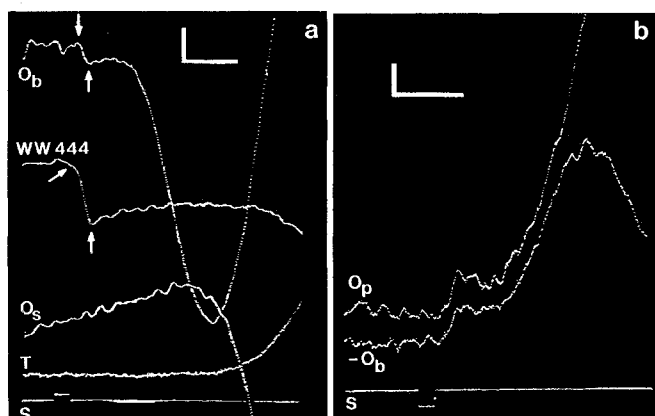


Fig. 1 (left). (a) Birefringence and other optical signals from a rat ventricular trabecula in normal Tyrode's solution at 24°C. The rate of stimulation and signal averaging was 20 per minute. Increasing light intensity is upward. The first component of the birefringence signal and the (action potential upstroke-related) dye signal are marked by arrows. Symbols: O_b , birefringence signal with polarizer and analyzer at 90° (5×10^{-4} , 25 sweeps); WW 444, 628-nm (30-nm half-amplitude bandwidth) nonpolarized light signal after staining the muscle with WW 444 (1 μ g/ml) for 20 minutes (5.3×10^{-4} , 10 sweeps); O_s , transmitted, nonpolarized white (scattered) light signal (1.8×10^{-4} , 8 sweeps); T , tension (0.12 mg); S , stimulus artifact. The time calibration bars are 4 msec. The intensity change in the optical calibrations was normalized to the resting intensity ($\Delta I/I_R$). The slow drift in trace O_s was a function of the analog track-and-hold circuit and could not always be eliminated. Birefringence and scattered light signals were always recorded before staining the fiber with dye. (b) Comparison of retarded and nonretarded light. Although the resting intensities (I_R) differ by a factor of 2.5, the changes in intensity (ΔI) nearly superimpose until movement artifact begins. $-O_b$, birefringence signal as in (a) but electronically inverted (5×10^{-4} , 25 sweeps); O_p , optical signal with the polarizer and analyzer axes at 0° (that is, parallel, 1.9×10^{-4} , 25 sweeps); S , stimulus artifact. Increasing light intensity is upward for O_p but downward for $-O_b$.

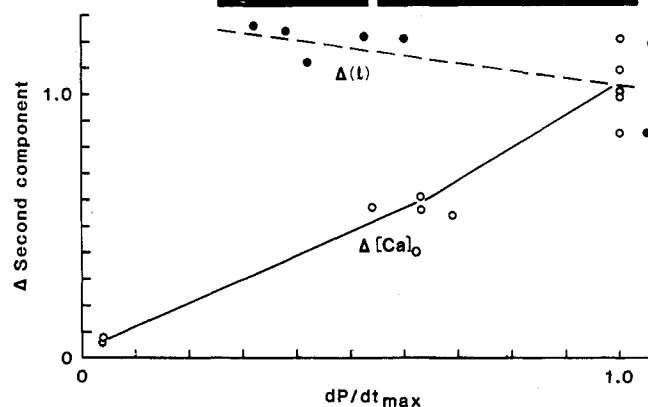
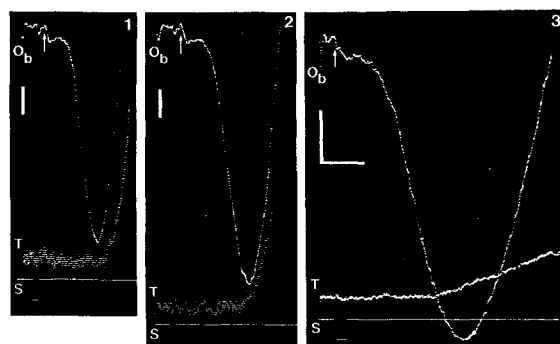


Fig. 2 (right). The relation of the second component of the birefringence signal from a rat ventricular trabecula to the maximum rate of tension development during a twitch, dP/dt_{max} , as influenced by changes of $[Ca]_o$, $\Delta[Ca]_o$, and by changes of muscle rest length, $\Delta(l)$. On the ordinate, Δ second component is the relative intensity change, $\Delta I/I_R$, of the second component taken 6 msec after the foot of the action potential upstroke. The values of Δ second component and dP/dt_{max} are normalized to the mean value for $[Ca]_o = 2.4$ mM. Panels 1, 2, and 3 illustrate the birefringence signals recorded in 2.4, 1.2, and 0.18 mM Ca^{2+} , respectively, at the same control rest length. The arrow in each panel marks the start of the action potential. The vertical calibration is 5×10^{-4} for optical traces and increasing intensity is upward. Signal averaging was 25 sweeps in panels 1 and 2 and 50 sweeps in panel 3. Tension traces (uncalibrated) are 10 sweeps each. Time calibration is 8 msec for all traces. In 0.18 mM Ca^{2+} , Tyrode's 1 mM MgCl₂ was added to the solution.

(wavelength = 632.8 nm) diffraction pattern from rat ventricular trabeculae were compared to the transmitted incandescent light (scattered light) signal. Under varied $[Ca]_o$ or addition of epinephrine, the laser zero intensity and the first-order diffraction peak changed at almost the same time as that of the scattered light signal (uncertainty < 1 msec). In the same preparations the onset of isometric contraction was found to lag behind those optical signals by slightly more than 1 msec. In Fig. 1a the sudden change in the scattered light signal (trace O_s) marks the time at which the birefringence signal is altered by movement artifact.

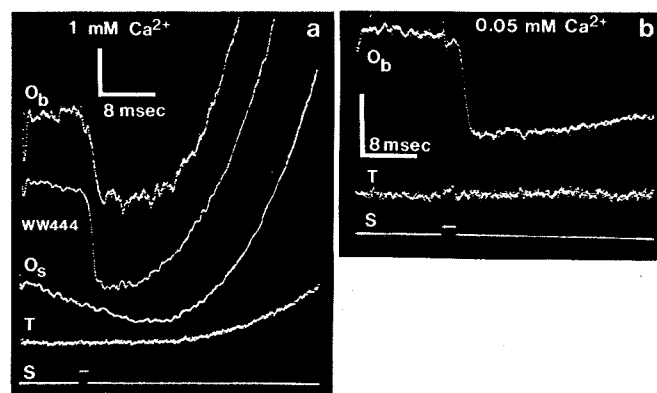
Figure 2 shows that the relative magnitude of the second component of the birefringence signal at a fixed time (6 msec) after the onset of action potential upstroke could be correlated to the maximum rate of tension development (dP/dt_{max}) in various $[Ca]_o$ (graph, open circles). However, little or no correlation of these two parameters was observed when dP/dt_{max} was altered two- to threefold by varying the resting length of the muscle (closed circles). Panels 1, 2, and 3 show the experimental recordings of the birefringence signal and isometric contraction in three different $[Ca]_o$. Increasing $[Ca]_o$ caused an increase in the rate of rise of the second component. The second component of the birefringence signal was found to be significantly potentiated by addition of epinephrine ($10^{-7}M$) in rat and guinea pig ventricular muscle.

A comparison of the ultrastructure of frog and mammalian myocardium indicates that the SR in frog heart is less abundant and more rudimentary than in the mammalian heart (10-12). Although frog atrium and ventricle are devoid of a T-tubular system there is also no T-system in some mammalian atria [as in cat (13) and guinea pig (14)]. Thus, the second component of the birefringence signal cannot be attributed to the T-system per se.

There is also evidence for a difference in the function of SR in frog and mammalian hearts from electromechanical studies. Voltage clamp experiments with mammalian heart indicate that phasic contraction (twitch) may result in part from a "triggered" release of Ca^{2+} from an intracellular source (15, 16). Positive inotropic and relaxant effects of epinephrine and postextrasystolic potentiation have been attributed to the alterations of the recirculated fraction of Ca^{2+} in the internal stores (16).

In agreement with these findings, the second component of the birefringence signal is present only in those tissues

Fig. 3. Optical signals from a frog atrial trabecula. (a) O_b , birefringence signal (5×10^{-4} , 50 sweeps); WW 444, 628-nm non-polarized light signal after staining the muscle with WW 444 ($2 \mu g/ml$) for 20 minutes (1×10^{-3}); O_s , transmitted nonpolarized white (scattered) light signal (4×10^{-4} , 25 sweeps); T, tension (0.65 mg); S, stimulus artifact. Birefringence and scattered light signals were taken before staining the muscle with dye. There is a slow baseline drift on O_s (see legend to Fig. 1a). (b) Signals in 0.05 mM Ca^{2+} Ringer solution; O_b (1.9×10^{-4} , 50 sweeps); T (0.16 mg). Note that the second component is absent in the frog heart.



which demonstrate an internally releasable Ca^{2+} store. In fact, the relative magnitude or the rate of rise of the signal is altered by $[Ca]_o$ and epinephrine (Fig. 2) in a manner compatible with the effect of these agents on releasable Ca^{2+} pools.

Our results (Fig. 3) are also consistent with previously published findings that in frog heart Ca^{2+} enters the cell under direct and continuous membrane potential control (16) and that there is no internal releasable Ca^{2+} store. Modulators of SR activity such as caffeine and epinephrine failed to reveal a second component of the birefringence signal in the frog heart. Additional evidence supportive of our contention that the second component is related to Ca^{2+} release from the SR comes from experiments with skinned cardiac fibers in which internal release of Ca^{2+} was found in mammalian but not frog hearts (17).

In evaluating the nature of the birefringence signal which precedes the development of tension in mammalian heart, it is clear that the first component monitors the action potential. Our evidence is based on comparison of the time course of the first component with that of the voltage-sensitive dye signal from WW 444 in both mammalian and frog hearts (Figs. 1 and 3).

The second component of the birefringence signal, associated in heart and skeletal muscle with SR activity, may arise from a potential change across the SR membrane. Comparisons of the birefringence signal with membrane potential-sensitive dye signals [WW 781 and diIC₁ (5)] in skeletal muscle have shown several cases where the signals are similar (5, 6). The second component of the birefringence signal in skeletal fibers has been described as occurring simultaneously with the Ca^{2+} -related signal of the calcium-indicator dye arsenazo III (7). Therefore, if an SR membrane potential change occurs, it could be gen-

erated by calcium release from the SR.

Implicit in the description of birefringence is that the orientation of a structure that retards polarized light must be regular about some axis (18). The regular array of the SR membranes within the muscle cells fulfills this requirement. It is also possible that proteins in the SR membrane have as much net orientation as the SR membrane itself. One such protein is the Ca^{2+} -dependent adenosinetriphosphatase which has been associated with the SR membrane in freeze-fracture studies and with the calcium reuptake system (19). Calcium binding to this protein could induce molecular changes giving rise to retardation changes.

Other structures in myocardium which could be implicated in the genesis of the second component are the highly oriented contractile proteins. We think, however, that the contractile proteins are an unlikely source of a second birefringence signal because (i) the myofibrillar content of the frog and mammalian heart are similar, with 54 percent (volume) for frog atrium (20) and 45 percent for rat ventricle (12), yet the signal is absent in frog heart (compare Figs. 1 and 3); and (ii) the myofilament sensitivity of frog and mammalian ventricle to Ca^{2+} in skinned fibers does not seem to be different.

We think, therefore, that the species differences with respect to the second birefringence signal occurring in parallel with the presence of releasable Ca^{2+} stores in mammalian hearts strongly suggests that the second component of the birefringence signal reflects a step in excitation-contraction coupling that is probably related to Ca^{2+} release from the SR.

R. WEISS
M. MORAD

Department of Physiology,
University of Pennsylvania,
Philadelphia 19104

References and Notes

1. L. B. Cohen, B. Hille, R. D. Keynes, *J. Physiol. (London)* **211**, 495 (1970).
2. _____, *ibid.* **203**, 489 (1969).
3. S. M. Baylor and H. Oetliker, *ibid.* **264**, 141 (1977).
4. _____, *Nature (London)* **253**, 97 (1975).
5. H. Oetliker, S. M. Baylor, W. K. Chandler, *ibid.* **257**, 693 (1975).
6. S. M. Baylor, W. K. Chandler, M. M. Marshall, in *Muscle Contraction: Excitation-Contraction Coupling*, A. D. Grinnel and M. A. B. Brazier, Eds. (Academic Press, New York, 1981).
7. S. M. Baylor, M. M. Marshall, W. K. Chandler, *Biophysics (USSR)* **25**, 119a (1979).
8. R. K. Gupta, A. Grinvald, L. B. Cohen, K. Kamino, F. Leshner, M. B. Boyle, A. F. Waggoner, C. H. Wang, *J. Membr. Biol.* **58**, 123 (1981).
9. A. Eberstein and A. Rosenfalck, *Acta. Physiol. Scand.* **57**, 144 (1963).
10. S. Page and R. Niedergerke, *J. Cell Sci.* **2**, 179 (1972).
11. S. R. Sommer and E. A. Johnson, *Z. Zellforsch. Mikrosk. Anat.* **98**, 437 (1969).
12. E. Page, L. P. McCallister, B. Power, *Proc. Natl. Acad. Sci. U.S.A.* **68**, 1465 (1971).
13. N. S. McKnutt and D. W. Fawcett, *J. Cell Biol.* **42**, 46 (1969).
14. N. Sperelakis and R. Rubio, *J. Mol. Cell Cardiol.* **2**, 211 (1971).
15. E. H. Wood, R. L. Heppner, S. Weidmann, *Circ. Res.* **24**, 409 (1969).
16. M. Morad and Y. Goldman, *Prog. Biophys. Mol. Biol.* **27**, 257 (1973).
17. A. Fabiato and F. Fabiato, *Ann. N.Y. Acad. Sci.* **307**, 491 (1978).
18. H. S. Bennet, in *McClung's Handbook of Microscopical Techniques*, R. McClung Jones, Ed. (Hoebner, New York, 1950), pp. 591.
19. C. Franzini-Armstrong, *Fed. Proc. Fed. Am. Soc. Exp. Biol.* **34**, 1382 (1975).
20. B. Eisenberg, personal communication.
21. We thank S. Baylor for helpful criticisms in the preparation of this manuscript.

22 December 1980; revised 23 April 1981

Collagen α B Chain: Increased Proportion in Human Atherosclerosis

Abstract. In a study of human atherosclerotic plaques, the relative abundance of α chains in pepsin-solubilized collagens from 28 human aortas was estimated by sodium dodecyl sulfate-polyacrylamide gel electrophoresis. The ratio of α B, a component of the α chain in type V collagen, to α 1(I) was markedly increased in the atherosclerotic plaques compared to the nonsclerotic intact media and adventitia. It is suggested that proliferating smooth muscle cells in the sclerotic lesion were transformed to synthesize a larger amount of collagen α B chain during the process of human atherogenesis.

Fibrous thickening of the intima with lipid deposition is the main feature of human atherosclerosis. Collagen is a major component of human atherosclerotic plaques, constituting as much as 30 percent of the dry weight (1). At present at least five genetically distinct species of collagen are known (2). Type I collagen, designated $[\alpha$ 1(I)]₂ α 2, is the most common collagen (3). Type II (4) and III collagens (5) consist of three identical α chains and are designated as $[\alpha$ 1(II)]₃ and $[\alpha$ 1(III)]₃, respectively. Type II collagen is found exclusively in cartilagi-

nous tissue. Type III collagen, observed as fine reticulin fibers, is found in several tissues such as skin, aorta, and uterus. Type IV collagen is the basement membrane collagen and a molecular formula $[\alpha$ 1(IV)]₃ has been popular (6), but there still remains some controversy (2). Type V collagen is made up of α A and α B (7) or A and B chains (8). This collagen is synthesized by a variety of cells including smooth muscle cells (9, 10) and tends to be localized pericellularly (10). Blood vessels contain types I, III, IV, and V collagens. Type III collagen is the pre-

dominant collagen of nonsclerotic media of the human aorta, comprising approximately 70 percent of the total collagen (11). However, only a few reports are available concerning the change of collagen types in human atherosclerosis (10-12). The present study was undertaken to determine the compositional change of collagen types by estimating relative proportions of collagen α chains. Here I report that the α B chain of type V collagen is proportionately increased in human atherosclerotic plaques.

Twenty-eight aortas were obtained at autopsy from humans (ages 54 to 68 years) who had died of various diseases including stroke, myocardial infarct, aortic aneurysm, and neoplasms. Aortas were removed within 4 hours after death, samples being collected from portions with sclerotic lesions. (All of the aortas showed atherosclerotic lesions at some stage of development.) Samples of adjacent intact media and adventitia were used as controls. Fragments of all of the samples were fixed in 10 percent Formalin for histological study. Minced tissues were washed in cold distilled water overnight and freed of blood. Tissues were homogenized with a Polytron ST-10 in 50 volumes of 0.5M acetic acid containing pepsin (Sigma, twice crystallized) at a concentration of 1 mg/ml. Collagen was extracted with constant stirring for 24 hours at 4°C. The solutions were centrifuged at 39,000g for 1 hour at 4°C. Collagen was reextracted from the pellets under the same conditions for 48 hours. The supernatants were then combined and collagen was precipitated by adding 4.0M NaCl to a final concentration of 2.0M. The precipitate was dissolved in 0.5M acetic acid and dialyzed against 0.02M Na₂HPO₄. Precipitated collagen was redissolved in 0.5M acetic acid, then

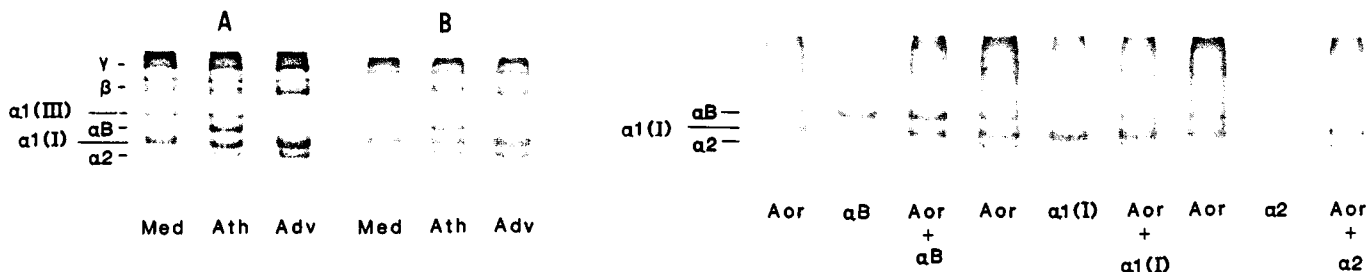


Fig. 1 (left). Sodium dodecyl sulfate (SDS)-polyacrylamide gel electrophoresis of pepsin-solubilized collagens from the intact media (Med), atherosclerotic plaque (Ath), and adventitia (Adv) of the human aorta. (A) Samples of heat-denatured collagen (20 to 30 μ g) were electrophoresed on the SDS-polyacrylamide gel slab for 2.5 hours. One hour after reduction in situ with β -mercaptoethanol the electrophoresis was resumed for another 2.5 hours. (B) Electrophoresis of the same samples as above for 5 hours without reduction with β -mercaptoethanol. Since reduction in situ did not change the electrophoretic behavior of α B, α 1(I), and α 2, these chains were not held by disulfide bonds. In this study the α chains derived from type IV collagen could not be detected because of their paucity in the sample. Fig. 2 (right). Sodium dodecyl sulfate (SDS)-polyacrylamide gel electrophoresis of the aortic collagen (Aor) and its component α chains. Samples (20 to 30 μ g) of aortic collagen, purified α chains, and a mixture of the two were electrophoresed on the SDS-polyacrylamide gel slab for 5 hours without reduction with β -mercaptoethanol. Note that purified α B, α 1(I), and α 2 comigrate with corresponding α chains in the aortic collagen. See the text and legend to Fig. 1 for details.